RESEARCH ARTICLE

The Effects of Curcumin on Hyperglycaemia-Induced Optic Nerve Damage in Wistar Albino Rats: An Electron Microscopic and Stereological Study

İ.O. Şahin[1], M.B. Tunalı[2*], A. Aktaş[2], K.K. Tüfekci[3] and S. Kaplan[1]

[1]Department of Histology and Embryology, Ondokuz Mayıs University, Samsun, Türkiye; [2]Department of Histology and Embryology, Faculty of Veterinary Medicine, Istanbul University-Cerrahpasa, Istanbul, Türkiye; [3]Department of Histology and Embryology, Faculty of Medicine, Kastamonu University, Kastamonu, Türkiye
*Corresponding author: basaktunali@iuc.edu.tr

A B S T R A C T

This study examined potential therapeutic or preventive benefits of curcumin on the damage caused by hyperglycemia to the optic nerves of diabetic rats. Forty-two Wistar female albino rats were allocated to 7 groups at random, with 6 rats in each group. The rats of control group (Cont) were not subjected to any treatment. Corn oil (1ml/kg) was applied to Sham group (Sham) via gavage for 14 days. For the diabetes model, rats of four groups were given one dose of 50 mg/kg streptozotocin (STZ) intraperitoneally. The diabetic animals received gavage treatments of 30 mg/kg curcumin in corn oil for 14 days. Curcumin and STZ were applied simultaneously in the diabetes-curcumin 3 (DC3) group. Curcumin was given to the diabetes-curcumin 1 (DC1) group 7 days and to the diabetes-curcumin 2 (DC2) group 21 days after the diabetes model was created. The curcumin (Cur) group received just curcumin (30 mg/kg) in corn oil for 14 days). Histopathological analysis was performed on semi-thin (500 nm) sections. In thin (70 nm) sections, quantitative parameters of optic nerve were examined by stereological methods. Diabetes significantly reduced the number of myelinated axons compared to the control group (p<0.05). The DC2 group compared to the diabetes group had higher myelinated axons number (p<0.05). The effect of curcumin application on optic nerve of diabetic animals did not show any difference in other parameters. Qualitative analysis showed morphological changes in optic nerve and protective effect of curcumin in ultrastructural analysis, suggesting its potential therapeutic role against diabetic optic nerve damage. The electron microscopic analysis revealed that the morphology of the nerve fibres was preserved in the Cur group in comparison to the control group.

INTRODUCTION

Diabetes mellitus (DM) is a complex metabolic disease characterized by hyperglycaemia and high glucagon levels (Tüfekci and Kaplan, 2023). This condition is caused by structural defects in the insulin molecule, as well as complete or partial insufficiency of pancreatic insulin output and insulin ineffectiveness (Conti *et al.,* 2017). This disease progresses with impairment in the metabolism of carbohydrates, proteins, and lipids, and requires multifactorial risk-lowering strategies beyond glycaemic control and continuous medical care. Pathogenesis of this disease is explained by absolute insulin deficiency in Type 1 DM and insulin secretion loss due to pathogenesis of β cells in Type 2

DM. Approximately 90-95% of all diabetic persons show type 2 diabetes mellitus. DM can cause changes during any phase of life, affecting other organs and systems in the body, leading to acute and chronic complications. Acute complications may be hypoglycaemia or hyperglycaemia, resulting in diabetic ketoacidosis and hyperglycaemic hyperosmolar status (Forbes and Cooper, 2013). Long-term DM causes changes in the vasoconstrictor-vasodilator balance and leads to impaired blood flow in the affected areas (Creager *et al.,* 2003). Patients with chronic diabetes may suffer from microvascular-related neuropathy, retinopathy, and nephropathy in the long term. It is defended that people who are suffering from diabetes need antioxidants more than others, considering that free radical formation

increases in diabetes and decreases in radical binding systems (Johansen *et al.,* 2005).

A significant part of the pathophysiology of diabetes and its consequences is attributed to oxidative stress (OS). The factors that cause OS to increase in diabetes are non-enzymatic glycosylation, autoxidative glycosylation, sorbitol pathway activity, various changes in antioxidant defence system and hypoxia. Antioxidants scavenge reactive oxygen species and/or block peroxidation chain reaction to prevent lipid peroxidation. Endogenous and exogenous antioxidants are two categories of antioxidants (Čolak *et al.,* 2017). Mitochondrial cytochrome oxidase, catalase, glutathione reductase (GR), Se-dependent glutathione peroxidase (GPx) and superoxide dismutase (SOD) are examples of enzyme-derived antioxidants. Non-enzymatic antioxidants include glutathione, ascorbic acid (vitamin C), β-carotene, melatonin, flavonoids, carotenoids, polyphenols, uric acid, cysteine, ceruloplasmin, curcumin, melatonin, bilirubin and polyamines (Čolak *et al.,* 2017; Qui, 2022).

Curcumin is an active constituent of turmeric and widely used in traditional medicine. It has anti-hyperglycaemic properties working against diabetes mellitus and shows antioxidant and neuroprotective effects on diabetic complications with therapeutic and protective properties that have been shown in many studies (Aşıcı *et al.,* 2021). This compound exhibits therapeutic effects, especially in diabetic neuropathy (DNp), which is one of the common complications of diabetes (Jia *et al.,* 2017). In addition to DNp affecting the central and peripheral nervous system, curcumin is known to be the preferred therapeutic substance for many brain diseases due to its ability to cross capillary wall in the system (Kalani *et al.,* 2014). According to Kaplan *et al.* (2023), the use of the curcumin and blueberry may represent a supportive approach to the protection of nerve fibers after peripheral nerve crush injury.

While most of the previous studies focused on the peripheral nerves in diabetic neuropathy, studies on how the optic nerve, which is a component of the central nervous system, was affected by the diabetes process are insufficient. This study aimed to examine the effects of diabetes on optic nerve and to evaluate possible therapeutic effects of curcumin by using electron microscopic and stereological methods.

MATERIALS AND METHODS

Animals and groups: A total of 42 Wistar albino female adult rats, aged 12 weeks with body weight of 250-300g were used in the study. Experimental rats were provided by the university animal house. The protocols and experiments were authorized by the Animal Care and Ethics Committee of Ondokuz Mayıs University (HADYEK 2017-53 and 30.03.2018). Experimental rats were kept under an environment of 12 hours light-dark cycle, ambient temperature of 22±2°C with 45-50% relative humidity, conventional conditions, and were provided with ad libitum standard commercial chow feed and water.

These rats were randomly divided into seven equal groups, with six rats in each group. The rats of control group (Cont) were not subjected to any treatment during experimental period. Corn oil (1ml/kg) was given to rats of Sham group (Sham) via gavage for 14 days. Streptozocin was injected intraperitoneally (a single dose of 50 mg/kg) to induce diabetes mellitus in rats of four groups (DM groups). Curcumin (30 mg/kg) was dissolved in corn oil and given to the diabetes groups 7 days later (DC1), 21 days later (DC2) and simultaneously with streptozocin (DC3). The animals in the Cur group were given the same amount of curcumin dissolved in corn oil for 14 days via intragastric gavage. An inclusion criterion to study for diabetic subjects was determined based on the previous study (Tufekci and Kaplan, 2023).

Tissue collection and analysis: Thirty-five days after induction of diabetes (start of the experiment), animals were anesthetized and intracardiac perfusion was performed, as described in a previous study (Tufekci and Kaplan, 2023). After the perfusion process ended, bilateral optic nerve tissues were removed, and right optic nerve tissue samples were subjected to processing for electron microscopy. Resin embedded tissue samples were used for stereological and histopathological analysis on images obtained via electron microscope. Sections of 70 nm were taken on a 200-mesh copper grid using the ultra-microtome and subjected to contrasting for electron microscopic analysis (Tufekci and Kaplan, 2023). Sections of 500 nm were taken on a glass slide and stained with toluidine blue stain (Tufekci *et al.,* 2023).

Stereological analysis: The optic nerve cross-sectional areas were analysed in the ImageJ program with the help of the camera-attachment Olympus microscope (BX43). Optic nerve cross-sectional areas were estimated by encircling them with ImageJ program at 10X magnification under the light microscope. Images for analysis of thin sections were obtained in a transmission EM (JEOL JSM-7001F, JEOL Ltd.). Images from the optic nerve cross-sectional areas were taken from the grid mesh in the electron microscope sequentially as far as possible. The systematic random sampling rule was applied to these EM images as far as possible; since some sampled area was occupied by grid bars, pictures of the next area were taken. All calculations were made with ImageJ program.

The optic nerve was evaluated using stereological methods, as explained in the previous study (Tufekci *et al.,* 2023). Density of axon number calculation was made using unbiased counting frame from pictures taken from the image area. The optic nerve cross-sectional area of that animal was multiplied with the average myelinated axon number density value obtained from the optic nerve of each animal and the total axon number of the relevant animal was calculated. The formula for the estimation is given below:

N (total axon number) = Density of axon number x Area of optic nerve cross section

The axon area was determined by encircling the area of the axon, which corresponded to a point determined by a grid in each image. Analysis was made for axons at the same point using the same grid in each image. This process was repeated by determining three axons at three different

points. The average of these three axon fields was obtained. In these axons, myelin sheath thicknesses were determined for each axon and four edges were obtained. By taking the average of these, myelin sheath thicknesses were obtained for each image (Tufekci *et al.,* 2023). Moreover, the coefficient of variance (CV) and coefficient of error (CE) were calculated to ensure the accuracy of the stereological design. These CE and CV values were acceptable according to the literature.

Statistical analysis: The data were statistically analysed using the SPSS software (version 21.0). The mean (±SE) was used to express the data. Shapiro-Wilk test was applied to determine whether the data were suitable for normal distribution. One-way analysis of variance (ANOVA) and Tukey's test were used for multiple means comparison because all the data showed a normal distribution. Value with p<0.05 was deemed statistically significant.

RESULTS

Stereological results: Myelinated axon number: Statistical evaluation of myelinated axon number showed significant differences among the groups. Compared to the control group, there was a significant decrease in myelinated axon number in the Sham, DM, DC1 and DC3 groups (p<0.01). Compared to Cur group, there was a significant decrease in Sham, DM, DC1 and DC3 groups (p<0.01). The myelinated axon number of the DC2 group increased significantly compared to the DC1 group (p<0.05) and DC3 and DM (p<0.01) groups (Fig. 1a).

Myelinated axon area: Statistical evaluation of myelinated axonal area also showed significant differences among the groups. Compared to the control group, a significant decrease in myelinated axonal area was recorded in the DC1 (p<0.01) and Cur (p<0.05) groups. A significant decrease (p<0.01) in the DC1 group compared to the Sham group was found (Fig. 1b).

Myelin sheath thickness: No significant difference of myelin sheath thickness was found among experimental groups (Fig. 1c).

Histopathological results:
Control Group: When the sections taken from the control group were examined under an electron microscope, it was observed that different sizes of the nerve fibres with normal myelin sheath and the cytoplasmic extension of the astrocyte surrounding them like a package had normal structure (Fig. 2a & 2b). When the optic nerve sections were examined at high magnifications, the morphologically intact state of the myelin sheath lamellae showed that these structures were well protected (Fig. 2c & 2d).

Sham Group: It was observed that the optic nerve tissue had partly preserved its morphological structure in electron microscopic images belonging to the Sham group Fig. 3a). Although the myelin sheath around the axons was normal in most areas, but it was noticed that the myelin sheath lamellae were separated from each other in some areas in the optic nerve (Fig. 3b). Astrocytic septa were of normal structure and thickness (Fig. 3c).
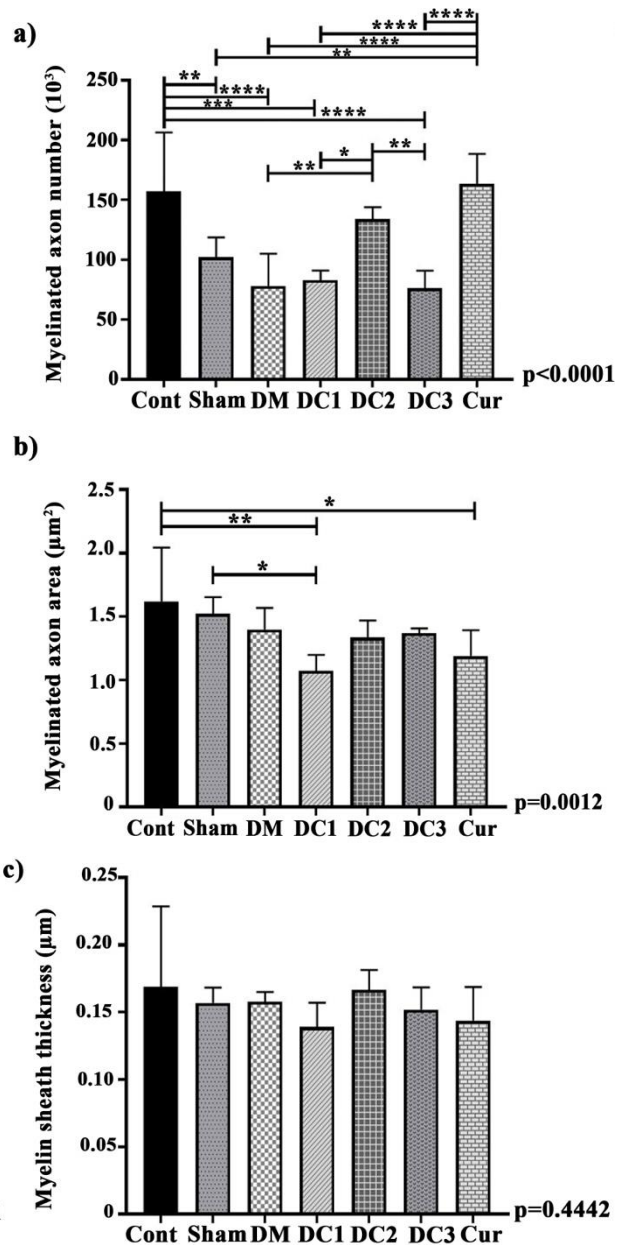

Fig. 1: (a): Myelinated axon number. Compared to the control group, there was a significant decrease in Sham (p<0.0090), DM (p<0.0001), DC1 (p<0.0002) and DC3 (p<0.0001) groups. Compared to the Cur group, there was a significant decrease of nerve fibres in the Sham (p<0.0027), DM (p<0.0001), DC1 (p<0.0001) and DC3 (p<0.0001) groups. Total nerve fibres of the DC2 group were significantly high compared to the DC1 (p<0.0192), DC3 (p<0.0056) and DM (p<0.0080) groups. **(b):** Myelinated axon area. Compared to the control group, there was a significant decrease in the DC1 (p <0.0011) and Cur (p <0.0165) groups. There was a significant decrease in the DC1 group compared to the Sham group (p <0.0110). **(c):** Myelin sheath thickness.

DM Group: Sections of the optic nerve belonging to the DM group were evaluated on the electron microscope (Fig. 4). The DM group showed that the nerve tissue had impaired morphological structure (Fig. 4a & 4b). In most areas, it was noticed that the myelin sheath around the myelinated axons lost normal morphology, since the lamellar structure of the myelin sheath was severely damaged, and even in some nerve fibres, the myelin sheath had lost its integrity completely and the regular myelin sheath lamellae were seen in minimal areas. In addition, vacuolization and the separation of the myelin sheath into

layers were very pronounced. Mainly, it was noticed that the myelin sheath around the large-calibrated nerve fibres was not in normal structure. On the other hand, the myelin sheath lamellae were uniform in small-calibrated nerve fibres in limited areas (Fig. 4c & 4d).
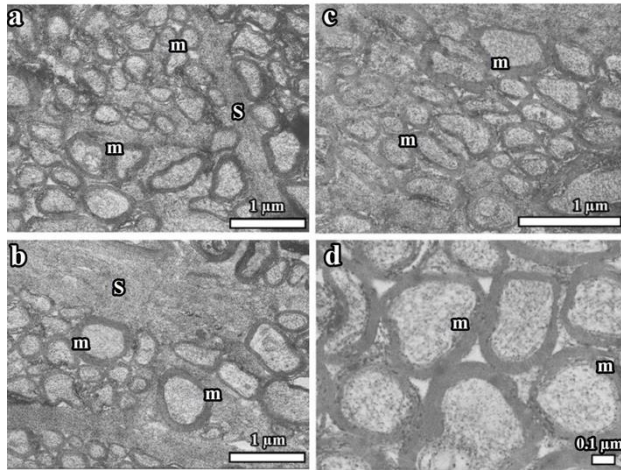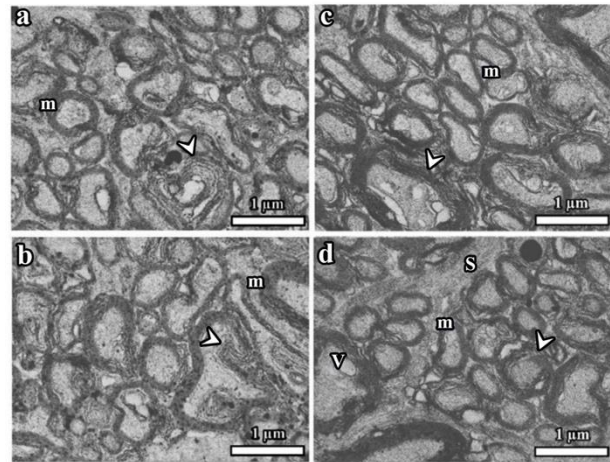

Fig. 2: The electron microscopic images of the sections taken from the optic nerve of the control group are observed. (**a, b**): It is noteworthy that large and small size diameter nerve fibres with properly organized myelin sheath (m) and astrocyte cytoplasmic (S) extensions surrounding them like a package are in normal structure. The smooth and tightly packed state of the myelin sheath lamellae shows that these structures are well protected. **(c, d):** At low and high magnification, large and small diameter nerve fibres with well-organized myelin sheath (m) are observed, respectively. The myelin sheath around the nerve fibres, which is the smooth and tightly packed state of the lamellae, is noteworthy. m: Myelin sheath; S: Astrocytic septa.
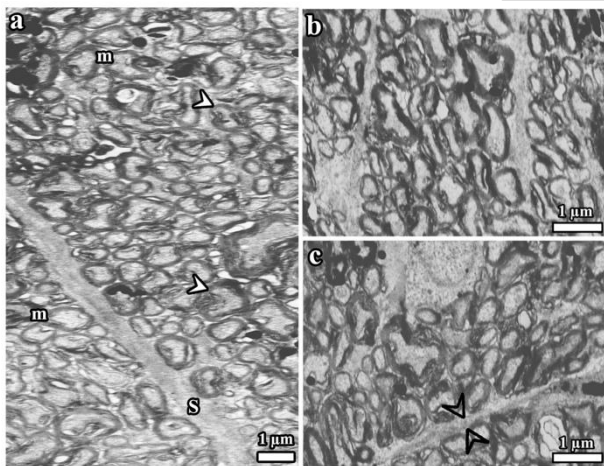
Fig. 3: Electron microscopic images of optic nerve were taken from the sham group. Tissue preserved its morphology. Although the myelin sheath (m) around the axons is standard in most areas, but it is noticed that the myelin sheath lamellae are separated from each other in some areas (arrowhead). **(a):** Astrocytic septa (S) have a normal structure and thickness, and vacuolization in the myelin sheath is seen (white arrowhead). **(b):** It was observed that the tissue preserved its structure, and although the myelin sheath around the axons is normal in most areas, it was noticed that the myelin sheath lamellae are separated from each other in some areas. **(c):** Astrocytic septa have a normal structure and thickness (black arrowhead). m: Myelin sheath; s: Astrocytic septa; arrowhead: Impaired myelin sheath.

DC1 Group: Electron microscopic images taken from optic nerve sections belonging to the DC1 group are shown in Fig. 5. The cytoplasmic extensions of the astrocytes surrounded the nerve fibres. In general, the
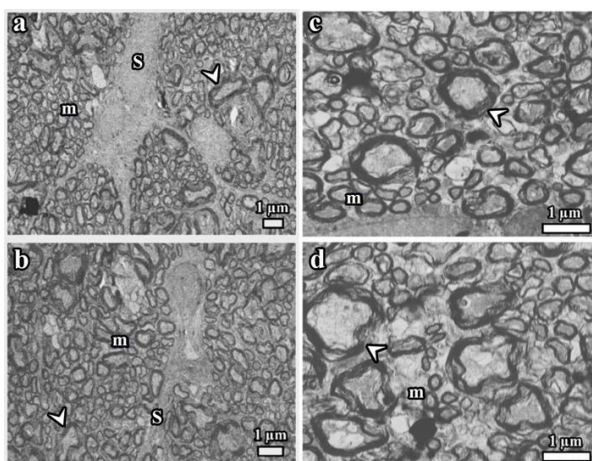
morphology of the fibres was preserved, and surrounding tissues and borders could be easily distinguished (Fig. 5a & 5b). While the myelin sheath surrounding the small-calibrated nerve fibres was better preserved in the small diameter fibres, the sheaths of the large, calibrated fibres were largely disrupted. It was seen that the cytoplasmic extensions of astrocytes had normal structure (Fig. 5c & 5d).
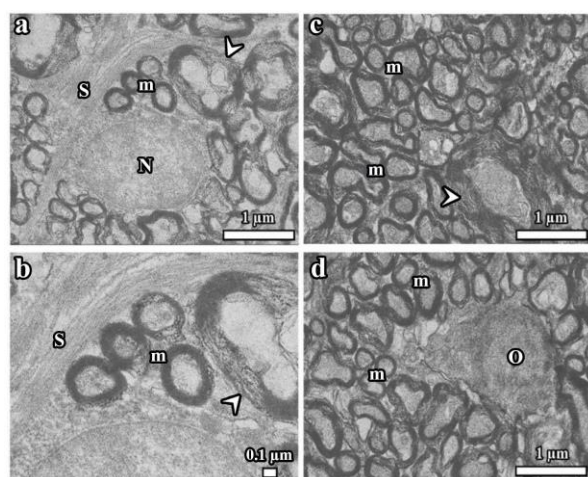

Fig. 4: Electron microscopic images taken from optic nerve sections belonging to the DM group showed that the tissue was not well protected in its morphology. **(a):** In most areas, it was noticed that the myelin sheath around the myelinated axons (m) was not in normal morphology. **(b):** It was observed that the lamellar structure of the myelin sheath was severely damaged (arrowhead), and even in some nerve fibres, the myelin sheath lost its integrity completely. Vacuolization and the division of the myelin sheath into layers draw attention. **(c):** The myelin sheath around the large-calibrated nerve fibres was not in normal structure (arrowhead), and the myelin sheath lamellae were uniform in small-calibrated nerve fibres in limited areas. **(d)** Cytoplasmic extensions of astrocyte (S) were prominent. The lamellar structure of the myelin sheath was damaged (arrowhead), and even in some nerve fibres, the myelin sheath lost its integrity completely. In addition, vacuolization was common between the sheath and axon, and the cleavage in the layers of the myelin sheath was noted. v: Vacuole; m: Myelin sheath; s: Astrocytic septa; Arrowhead: Disrupted myelin sheath.

DC2 Group: Electron microscopic images taken from optic nerve sections belonging to DC2 group were evaluated, as shown in Fig. 6. Myelinated axons of different diameters were observed in sections. Although most of the fibres were well protected, the presence of significant disruptions in the myelin sheath around some large diameter axons was noteworthy (Fig. 6a & 6b). Astrocyte and intermediate filaments of astrocyte were well seen. Oligodendroglia and optic nerve fibres looked to have normal morphology (Fig. 6c & 6d).

DC3 Group: Electron microscopic images taken from optic nerve sections belonging to the DC3 group are shown in Fig. 7. Severely damaged optic nerve axons, myelin sheaths, swollen vacuoles, astrocytes, and astrocyte extensions were common impairments (Fig. 7a & 7b). Notably, the large sizes of myelinated nerve fibres showed axon shrinkage and were gathered in the centre, whereas their myelin sheath remained intact. Thin astrocytic septa were observed in patches and among the nerve fibres; the thick and filamentous structure of the astrocytic septa was remarkable (Fig. 7c & 7d).
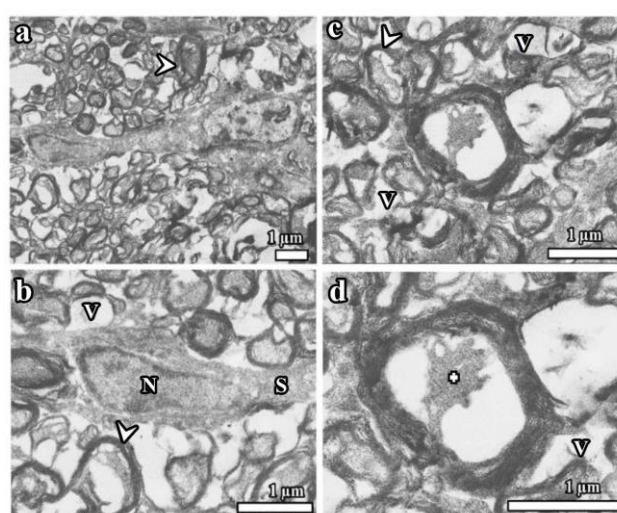
Fig. 5: Electron microscopic images taken from optic nerve sections belonging to the DC1 group are observed. **(a, b):** The cytoplasmic extensions of the astrocytes (S) surround the nerve fibres. In general, it was observed that the morphology of the fibres was preserved and that the surrounding tissues and borders could be distinguished. While the myelin sheath (m) surrounding the small-calibrated fibres was better preserved, it was noticed that the sheaths of the large-calibrated fibres were largely disrupted. **(c, d):** It is seen that the lamellae in the myelin sheaths of the large-calibrated fibres (arrowhead) are separated from each other, whereas the smaller-calibrated nerve fibres (m) are better protected. m: Myelin sheath; arrowhead: Impaired myelin sheath; S: Astrocytic septa.
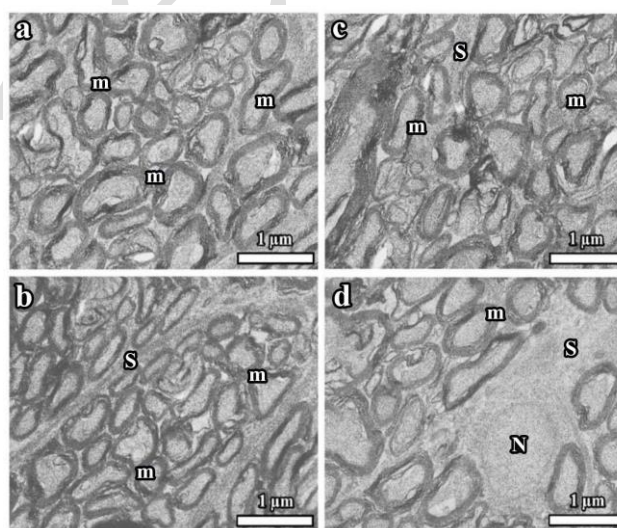

Fig. 6: Electron microscopic images taken from optic nerve sections belonging to the DC2 group are seen. **(a):** Axons of different diameters (m) are observed in sections. Although most of the fibres are well protected, the presence of significant disruptions in the myelin sheath around some large-diameter axons is noteworthy (arrowhead). Astrocyte and intermediate filaments of it are seen (S). Moderate to mild myelin sheath damage and swollen vacuoles separating the myelin sheath and axolemma are observed. **(b):** A magnified area of **(a)** is seen in detail. **(c):** Most nerve fibres were small in diameter. It was observed that the structures of these fibres were well preserved, but this was different with large-size fibres (arrowhead). **(d):** There is a centrally located oligodendroglia (O). m: Myelin sheath; arrowhead: Impaired myelin sheath; O: Oligodendrocyte nucleus; s: Astrocytic septa; N: Astrocyte nucleus.

Cur Group: Optic nerve sections belonging to the Cur group were evaluated (Fig. 8). Remarkably, most of the fibres observed in the section had normal morphology and showed the preserved structure of the astrocytic septa between the fibres (Fig. 8a & 8b). The fibres were tightly packed and in organized states and their normal axoplasm were seen. The nucleus and cytoplasmic extension of the astrocyte had a very healthy structure (Fig. 8c & 8d).

Fig. 7: Electron microscopic images taken from the optic nerve belonging to the DC3 group are seen. Severely damaged optic nerve axons, myelin sheaths, swollen vacuoles, astrocytes, and astrocyte extension are seen (arrowhead). **(a):** General structures of nerve fibres are magnified images of some part of **(a),** which are seen in **(b). (c):** The structures of most fibres in the nerve were disrupted, and many vacuoles (V) were formed between the fibres. Notably, in large-diameter nerve fibre, the axon contracts and collects in the centre (+), whereas the myelin sheath remains intact. **(d):** A high magnification of **(c)** is seen. V: Vacuole; arrowhead: Impaired myelin sheath; (+): Withdrawal of axon; S: Astrocytic septa; N: Astrocyte nucleus.

Fig. 8: Electron microscopic images taken from optic nerve belonging to the Cur group are seen. **(a):** Remarkably, most of the fibres (m) observed in the section have normal morphology and preserved structure of the astrocytic septa (S) between the fibres. **(b):** The fibres' tightly packed and organized states and their normal axoplasm are observed. Thin astrocytic septa are noticed. **(c):** Notably, most of the fibres observed in the section have a normal structure and preserved morphology of the astrocytic septa between the fibres. **(d):** Nucleus and cytoplasmic extension of the astrocyte are observed. m: Myelin sheath; s: Astrocytic septa; N: Astrocyte nucleus.

DISCUSSION

The retinopathy and peripheral neuropathy caused by effects of diabetes on the optic nerve are adversely affecting quality of life. The nerve fibre layer begins to become thin even prior to the start of diabetic retinopathy, particularly in the superior portion of the retina (Yanoff and Sassani, 2009). A previous study reported loss of giant axons of the optic nerve in the distal part after six weeks of

diabetes (Fernandez *et al.,* 2012). Also, the axon number and axon area of the optic nerves exposed to diabetes showed a decreasing trend. In another study, only the loss of large fibres in the optic nerve was observed (Flores *et al.,* 2000). On the other hand, a non-significant decrease of axon number was found in diabetic group compared to the control group by Bui *et al.* (2009). Although these studies do not show a common opinion on the number of axons in diabetic subjects, in our study, the DM group exposed to diabetes showed a decrease of the myelinated axon number in the optic nerve compared to the control group. In our view, it is a situation that results in axonal loss with the inflammatory response mechanism caused by the damage due to diabetes, but further studies are needed for better understanding of these mechanisms.

The axons of optic nerve originating from retinal ganglion cells are characterized by three axon size categories; large, medium, and small, with the average diameter ranging from 0.2 to 3.0 microns in the rats (Goyal *et al.,* 2023). In a study of diabetic rats, a non-significant difference was found between the control group and the diabetes group in the nerve sectional areas taken from the proximal and distal parts of the optic nerve (Dorfman *et al.,* 2015). Our results also showed non-significant change in the axonal area when the diabetic animals and the control group were compared, which is consistent with the published literature. Studies on optic nerves from diabetes and glaucoma models have consistently demonstrated that small-sized axons are more resistant to damage than large axons, the latter often being the first affected (Fernandez *et al.,* 2012). Another factor that can cause a change of axon area is neurofilaments that make up the cytoskeleton of large axons. An increase in the number of swollen axons with neurofilament protein deposits in the diabetes group compared to the control group was shown in the retinas of diabetic rats using an immunohistochemical study (Gastinger *et al.,* 2001). The reason for the absence of a significant difference in the axonal area between the control and diabetes groups may be a result of the swelling of the accumulated neurofilaments in the remaining axons despite the large size of axons lost in the diabetic optic nerve.

Various studies have demonstrated changes caused by hyperglycaemia in myelin sheath thickness. In a previous study (Bui *et al.,* 2009), a significant decrease was found in the myelin sheath thickness when the optic nerves were analysed in the experimental animals 12 weeks after the diabetes was induced by STZ. In the study of Flores and Corredera (2018), the control group and the diabetes group, myelin sheath thickness was examined six and 12 weeks after the STZ injections. The myelin sheath thickness did not change significantly between the control and diabetes groups at both weeks. In our study, there was no significant change when we compared the animals of the diabetes group with the control group, in terms of the myelin sheath thickness (MST). The reason for the lack of statistically significant difference between the groups in terms of MST may be that the 35-day diabetic period may not be sufficient to create damage to the myelin sheath. This may come from many factors that contribute to axonal degeneration. However, axonal damage does not always occur secondary to demyelination. Axonopathy is associated with the attack of axons by inflammatory cells regardless of demyelination and the effect of secreted inflammatory cytokines and toxic species on axons (Kuhlmann *et al.,* 2002). In our study, the inflammatory response to diabetes may have resulted in axonal loss without myelin sheath impairment.

We found that the myelinated axon number in the DC2 group treated with curcumin after 21 days of diabetes initiation showed a significant increase in comparison to the DM group. However, such an effect in the DC1 and DC3 groups was not seen. These results indicate that, despite its therapeutic effects, curcumin treatment has different results, which needs to be clarified by molecular and immunohistochemical analyses.

The results of the DC2 group treated with curcumin after 21 days of diabetes induction might be due to a long period of diabetes in comparison to the other two groups (DC1 and DC3), increased OS in the DC2 group; and curcumin might respond in a better way to accumulated OS due to its antioxidant feature. This anticipated comment needs to be evaluated in detail. It is well known that curcumin controls OS by inhibiting ROS elements in diabetic rats due to its antioxidant properties, increasing protein carbonyls and inducing changes in antioxidant enzyme activities (Sathyabhama *et al.,* 2022).

STZ, a known inducer of cytochrome P450 1A2, may have accelerated curcumin metabolism, potentially limiting its bioavailability (Drugbank, 2020). A detail investigation is needed to fully understand the function of cytochrome P450 1A2 in the metabolism of both STZ and curcumin. Curcumin may contribute to neurogenesis in addition to its neuroprotective and neuro-regenerative effects.

When the results of the axonal area of the groups were compared, a significant decrease in the axonal area was found in the DC1 and in the Cur groups compared to the control group. Moreover, a decrease was also found in the axonal area in the DC1 group compared to the Sham group. Such results on the axonal area were expected for the DM group but were not seen; this point also needs to be further investigated.

It has been reported that curcumin causes volume changes in diabetic pancreatic beta cells by increasing the activation and opening of anion channels and thus causing chloride and water output from the cell, which results in a decrease in the volume of these cells (Kössler *et al.*, 2012). Such decrease in the Cur group might have come from the volume-reducer effect of curcumin. Interestingly, there was a significant difference between the control and the DC1 groups. Further studies are also needed to explain this discrepancy.

The comparison of myelin sheath thickness among different groups did not reveal any difference among groups. Oligodendrocytes might explain this and may be more resistant to diabetes (Fernyhough, 2015). On the other hand, it is known that myelin sheath is seriously affected during diabetic neuropathy. Determination of some possible protective mechanism of oligodendrocytes during diabetes also needs to be evaluated.

The axons in the myelinated nerve were frequently seen to be separated from the myelin sheaths in the diabetic group. High plasma galactose concentration creates a hyperosmolar perineural environment and increases the amount of glycogen in Schwann cells in the peripheral nervous system, which have similar functions of oligodendrocyte in the CNS. In addition, it can be assumed that these separations between

the axon and the myelin sheath may be an indicator of axonal dysfunction in the paranodal region of nerve fibres affected by diabetes.

Electron microscopic examinations showed that curcumin improved myelin sheath disorganization caused by diabetes. Although our histopathological observations confirmed the curcumin protection, but stereological analysis did not support this idea. Impairment of the optic nerve, such as collapsed myelin sheath, vacuolisation in the sheath and axon, and degeneration of fibres, was reduced by curcumin treatment based on morphological examination. We determined that degenerated nerve fibres in the optic nerves and impaired myelin structures were decreased at different time periods of curcumin exposure after the induction of experimental diabetes.

It was also found that curcumin exerted its therapeutic effects on the optic nerve of the DC2 group better than the DC1 group in terms of astrocytic septa and myelin sheaths. This shows that curcumin is more effective against the chronic effects of diabetes than acute effects, compared to the DC3 group, where STZ was administered simultaneously with curcumin. The precise mechanism underlying protective effects of curcumin on myelin remains unclear. Additionally, influence of curcumin on iron homeostasis as a potential mechanism of myelin protection warrants further investigation.

One of essential components for oligodendrocytes to produce myelin is iron. A significant source of iron for oligodendrocytes is ferritin; it is known that hypomyelination is a result of iron deficiency (Todorich *et al.,* 2011). Alteration of the iron state is seen after inflammation and curcumin supplementation may reduce the ferritin protein, thereby affecting this change to prevent or reverse myelin damage (Chin *et al.,* 2014). We think curcumin shows the healing effects of myelin disorganization through these and other similar mechanisms.

Conclusions: Diabetes mellitus, characterized by chronic hyperglycaemia, leads to complications like diabetic optic neuropathy, which can impair vision. Our histological and electron microscopic findings demonstrate a protective effect of curcumin on optic nerve morphology in diabetic rat model. However, because the stereological analysis results do not support the findings revealed by microscopic evaluation, new experiments are needed to definitively determine the protective effects of curcumin on optic nerve structure and function. Sample designs and methods of applying curcumin are needed to ensure its maximum bioavailability.

Disclosure statement: The authors declare no conflict of interest related to this study.

REFERENCES

Aşıcı GSE, Kiral F, Bayar I, *et al.,* 2021. Cytotoxic and apoptotic effects of curcumin on D-17 canine osteosarcoma cell line. Kafkas Üniv Vet Fak Derg 27:4.

Bui BV, Loeliger M, Thomas M, *et al.,* 2009. Investigating structural and biochemical correlates of ganglion cell dysfunction in streptozocin-induced diabetic rats. Exp Eye Res 88:1076-83.

Chin D, Huebbe P, Frank J, *et al.,* 2014. Curcumin may impair iron status when fed to mice for six months. Redox Biol 2:563-69.

Čolak E, Ignjatović S, Radosavljević A, *et al.,* 2017. The association of enzymatic and non-enzymatic antioxidant defense parameters with inflammatory markers in patients with exudative form of age-related macular degeneration. J Clin Biochem Nutr 60:100-107.

Conti C, Mennitto C, Di Francesco G, *et al.,* 2017. Clinical characteristics of diabetes mellitus and suicide risk. Front Psychiatry 8:1-7.

Creager MA, Lüscher TF, Cosentino F, *et al.,* 2003. Diabetes and vascular disease: Pathophysiology, clinical consequences, and medical therapy: Part I. Circulation 108:1527-32.

Dorfman D, Aranda ML and Rosenstein RE, 2015. Enriched environment protects the optic nerve from early diabetes-induced damage in adult rats. PLoS One 10(8): e0136637. doi: 10.1371/journal.pone.0136637.

Drugbank, 2020. https://www.drugbank.ca/drugs/DB11672/biointer actions#enzyme-tab.

Fernandez DC, Pasquini LA, Dorfman D, *et al.,* 2012. Early distal axonopathy of the visual pathway in experimental diabetes. Am J Pathol 180:303-13.

Fernyhough P, 2015. Mitochondrial dysfunction in diabetic neuropathy: A series of unfortunate metabolic events. Curr Diab Rep 15:89.

Flores RA and Corredera BM, 2018. Glial cells and retinal nerve fibres morphology in the optic nerves of streptozocin-induced hyperglycemic rats. J Ophthalmic Vis Res 13:433-38.

Flores RA, Corredera BM, Santana FO, *et al.,* 2000. Optic nerve fibres and experimental diabetes. Arch Soc Esp Oftalmol 75(5):315-20.

Forbes J and Cooper M, 2013. Mechanisms of diabetic complications. Physiol Rev 93(1):137-88.

Gastinger MJ, Belforte N, Khin SA, *et al.,* 2001. Abnormal centrifugal axons in streptozocin-diabetic rat retinas. Invest Ophthalmol Vis Sci 42:2679-85.

Goyal V, Read AT, Brown DM, *et al.,* 2023. Morphometric analysis of retinal ganglion cell axons in normal and glaucomatous Brown Norway rats optic nerves. Transl Vis Sci Technol. 12:1-16.

Jia T, Rao J, Zou L, *et al.,* 2017. Nanoparticle-encapsulated curcumin inhibits diabetic neuropathic pain involving the P2Y12 receptor in the dorsal root ganglia. Front Neurosci 11:755.

Johansen JS, Harris AK, Rychly DJ, *et al.,* 2005. Oxidative stress and the use of antioxidants in diabetes: Linking basic science to clinical practice. Cardiovasc Diabetol 4:5; doi: 10.1186/1475-2840-4-5.

Kalani A, Kamat PK, Chaturvedi P, *et al.,* 2014. Curcumin-primed exosomes mitigate endothelial cell dysfunction during hyperhomocysteinemia. Life Sci 107:1-7.

Kaplan AA, Onger ME and Kaplan S, 2023. The effects of curcumin and blueberry on axonal regeneration after peripheral nerve injury. J Chem Neuroanat 130: 102260: doi: 10.1016/j.jchemneu.2023.102260.

Kössler S, Nofziger C, Jakab M, *et al.,* 2012. Curcumin affects cell survival and cell volume regulation in human renal and intestinal cells. Toxicology 292:123-35.

Kuhlmann T, Lingfeld G, Bitsch A, *et al.,* 2002. Acute axonal damage in multiple sclerosis is most extensive in early disease stages and decreases over time. Brain 125:2202-12.

Qui NH, 2022. Recent advances of using polyphenols to extenuate oxidative stress in animal production: Evidence from poultry. Kafkas Üniv Vet Fak Derg 28:535-41.

Sathyabhama M, Priya Dharshini LC, Karthikeyan A, *et al.,* 2022. The credible role of curcumin in oxidative stress-mediated mitochondrial dysfunction in mammals. Biomolecules 12:1405.

Todorich B, Zhang X and Connor JR, 2011. H-ferritin is the major source of iron for oligodendrocytes. Glia 59(6):927-35.

Tufekci KK, Kaplan AA, Kaya A, *et al.,* 2023. The potential protective effects of melatonin and omega-3 on the male rat optic nerve exposed to 900 MHz electromagnetic radiation during the prenatal period. Int J Neurosci 133:1424-36.

Tufekci KK and Kaplan S, 2023. Beneficial effects of curcumin in the diabetic rat ovary: a stereological and biochemical study. Histochem Cell Biol 159(5):401-30.

Yanoff M and Sassani J, 2009. Diabetes Mellitus. In: Gabbedy R and Nash S (eds), Ocular Pathology. 6th ed. Philadelphia, Mosby Elsevier, pp:619-20.